Validity of extended field-of-view ultrasound imaging to evaluate quantity and quality of trunk skeletal muscles

Noriko I. Tanaka[1,2], Madoka Ogawa[3], Akito Yoshiko[4], Hiroshi Akima[1,2]

1. Research Center of Health, Physical Fitness and Sports, Nagoya University, Furo-cho, Chikusa-ku, Nagoya, Aichi 464-8601, Japan. tanaka-n@htc.nagoya-u.ac.jp
2. Graduate School of Education & Human Development, Nagoya University, 1 Furo-cho, Chikusa-ku, Nagoya, Aichi 464-8601, Japan
3. Department of Exercise Physiology, Nippon Sport Science University, 7-1-1 Fukasawa, Setagaya-ku, Tokyo 158-8508, Japan
4. School of International Liberal Studies, Chukyo University, 101 Tokodachi, Kaizu-cho, Toyota-shi, Aichi 470-0393, Japan.

Correspondence: Noriko I. Tanaka,
Research Center of Health, Physical Fitness and Sports, Nagoya University. Furo-cho, Chikusa-ku, Nagoya 464-8601, Japan. TEL.: +81-52-789-3948, FAX: +81-52-789-3957,
E-mail: tanaka-n@htc.nagoya-u.ac.jp

ABSTRACT

This study examined the validity of extended field-of-view (EFOV) ultrasound imaging for evaluating the quantity (cross-sectional area, CSA) and quality (accumulation of intramuscular fat) of trunk skeletal muscles (rectus abdominis, abdominal oblique, and erector spinae) using magnetic resonance imaging (MRI) as a reference. Thirty healthy young men participated in this study. Cross-sectional images of trunk at the height of the 3rd lumbar vertebra were acquired and compared by EFOV ultrasound imaging and MRI. As a result, no significant differences was observed in the CSAs by two methods ($0.74 \leq R^2 \leq 0.85$). Echo intensities significantly correlated with MRI-derived accumulation of intramuscular fat in each skeletal muscle group. However, the correlation coefficients were relatively low ($0.37 \leq r \leq 0.47$, $p<0.05$). These results indicated EFOV ultrasound imaging is a reliable method for assessing trunk skeletal muscle CSA. Further research is warranted to find the optimal ultrasound setting for evaluating muscle quality.

Keywords: cross-sectional area, echo intensity, intramuscular fat, panoramic image, trunk skeletal muscle, MRI

Introduction

The measurement of skeletal muscle mass is important for analyzing muscle strength and health.-Age-related losses in muscle strength and/or skeletal muscle mass are generally referred to as sarcopenia. Sarcopenia and accumulation of non-contractile tissue, such as intramuscular fat, with aging and/or inactivity have been implicated in the development of insulin resistivity (Lee et al. 2011; Sachs et al. 2019), physical dysfunction and the onset of low back pain (e.g., Hicks et al. 2005; Ryan and Harduarsingh-Permaul 2014). More than 40% of whole-body skeletal muscle volume is present in the trunk (Tanaka et al. 2007). Skeletal mass may decrease more in the trunk than in other body segments by aging and low back pain (Ishida et al. 1997; Teichtahl et al. 2015). We previously reported that the distribution of the trunk skeletal muscles, particularly for the abdominal oblique and iliopsoas may be affected by the changes in the visceral fat area (Tanaka et al. 2007, 2019). Therefore, quantitative and qualitative evaluations of trunk skeletal muscles are useful for the early diagnosis of sarcopenia (Cruz-Jentoft et al. 2010 and 2019) as well as type 2 diabetes. In fact, Ido et al. (2015) indicated that the abdominal muscle thickness is a more accurate indicator of sarcopenia and metabolic syndrome in obese patients.

Magnetic resonance imaging (MRI) and computed tomography (CT) are the gold standard tools for accurately assessing skeletal muscle mass. However, these methods are expensive and time consuming to analyze. Since CT involves exposure to X-rays, we cannot perform it on pregnant women or children. On the other hand, ultrasound imaging is a cheaper, quicker, safer, and more widely available technique compared with MRI and CT. However, its field of view is limited, therefore, it generally provides information on the thickness of tissues (e.g., Abe et al. 1994), not the cross-sectional area (CSA) of skeletal muscle. To overcome the limitation of a small field of view, extended field of view (EFOV) was developed using panoramic imaging technology. Another disadvantage of ultrasound imaging is that muscle quality cannot be represented as an absolute value or as a ratio of fat and/or fibrosis to muscle. Echo intensity is a qualitative index, not parameter, of skeletal muscle. Previous studies reported significant correlation between echo intensity and the contents of fat and fibrous tissue in skeletal muscle (Pillen et al. 2008 and 2009). Reimers et al. (1993) demonstrated that muscle echogenicity correlated with the content of intramuscular fat, but not fibrous tissue in humans. Akima et al. (2016) indicated that the echo intensity of thigh muscles assessed by ultrasound imaging was associated with the content of intramuscular adipose tissue measured by MRI and extramyocellular lipids by ^{1}H magnetic resonance spectroscopy. Collectively, echo intensity can provide qualitative information on a given muscle.

We recently reported the repeatability of EFOV ultrasound imaging to assess muscle CSA and echo intensity in the trunk (Tanaka et al. 2017). Similar to previous studies targeted limb skeletal muscles (e.g., Melvin et al. 2014), the intraclass correlation coefficient of EFOV ultrasound imaging to measure skeletal muscle CSA was “almost perfect” (Landis and Koch 1977), while echo intensity was “substantial” or “almost perfect” (Landis and Koch 1977). However, we were unable to confirm the validity of EFOV ultrasound imaging for measuring trunk tissue composition (Tanaka et al. 2017) due to the lack of CT or

MRI data. In addition, our other previous studies suggested that the distribution of some trunk skeletal muscles, particularly the abdominal oblique and iliopsoas muscles is affected by changes in the visceral area (Tanaka et al. 2007, 2019).Therefore, the purpose of the present study was to examine the validity of measurements of abdominal skeletal muscle CSA and echo intensity using EFOV ultrasound imaging with MRI as a reference. We hypothesized that ultrasound EFOV imaging is reliable for simultaneously evaluating the quantity and quality of abdominal skeletal muscles. Moreover, we speculated that the quantitative and/or qualitative characteristics of some abdominal skeletal muscles such as abdominal oblique correlate with the visceral fat area.

Materials and Methods

Subjects. Thirty healthy young men participated in the present study. The data was acquired from January to September in 2017. The subjects and images in this study were different from those in previous studies (Tanaka et al. 2017). For the recruitment of the applicants, we used leaflets in our University. None of the subjects had any previous medical history or illness during the investigation. Prior to the initiation of the investigation, each subject was informed about the experimental design and associated risks and discomforts, namely, the protection of privacy during abdominal image acquisition, orthostatic hypotension, and transient hypertension accompanying force development. Informed consent was obtained from all participants. The present study was approved by the Ethics Committee of the Research

Center of Health, Physical Fitness and Sports (27-13), and Graduate school of Medicine (2016-0254-5), Nagoya University and was performed in accordance with the Declaration of Helsinki. The sample size was calculated for correlations with an anticipated effect size: 0.5, desired statistical power level: 0.8, and probability level: 0.05 with G*Power software (Faul et al. 2009). The minimum sample size required was 26.

Procedures. Each participant visited the laboratory twice, one for MRI, the other for residual measurements, with1 to 6 days interval, at approximately the same time of day (± 1 h). The order of measurement day was random. Participants were instructed to keep a similar lifestyle between trials and refrain from excessive drinking and eating or any vigorous physical activity from 4 h before testing. Body weight and body fat were measured by ITO-InBody 370 (Ito Co., Ltd., Japan). Height and waist circumference were also measured by one experienced expert (M. O.).

MRI measurements. Cross-sectional images of the trunk at the height of the 3rd lumbar vertebra (L3) were acquired by MRI. A representative landscape for acquiring images was shown in Figure 1. Trunk MRI was performed using the 3T Siemens Magnetom Aera system (MAGNETOM Verio, Siemens Healthcare Diagnostics, Munich, Germany) with breath holding after inspiration for approximately 15 seconds. Ectopic fat accumulation in skeletal muscle and the intraperitoneal area was evaluated on MRI using the fat-water separated two-point Dixon imaging technique, which uses a chemical shift between the resonance frequencies of protons bound in fat and water. The sequences were followings; repetition time: 4.5 ms, echo time: 1.225 and 2.45 ms, flip angle: 9°, FOV: 320*512 mm, Matrix size: 255*255, slice thickness: 0.5 cm, slice interval: 0 cm. These images were used as reference values for the quantity and quality of the abdominal skeletal muscle groups in the present study.

Ultrasound measurements. In each trial, participants lay on a bed. Then a portable B-mode ultrasound device (Logiq e, GE Healthcare Co., Ltd., USA), using a linear-array probe (12L-RS, GE Healthcare Co., Ltd., USA), was applied to obtain cross-sectional images of the trunk skeletal muscles at the height of L3. Ultrasound settings (Frequency: 8 Hz, Gain: 90 dB, Depth: 8 cm, focus: top of the image, brightness: middle of the settable range) were consistent for each scan. Detailed information on measurement methods were described elsewhere (Tanaka et al. 2017). We used LogicViewTM software (GE Health Care Co., Ltd., USA) to generate EFOV images. We acquired cross-sectional images of the rectus abdominis, abdominal oblique (the sum of the internal oblique, external oblique, and transversus abdominis muscles), and low back (the sum of the longissimus dorsi, iliocostal, semispinal, and quadratus lumborum muscles) muscle groups from each subject (Figure 1). Similar to the previous studies (e.g., Ahtiainen et al. 2010), we scanned until three EFOV ultrasound images of sufficient quality were obtained. One experienced expert (N.T.) performed all ultrasound measurements.

Image analysis. All MR images were analyzed using SliceOmatic 5.0 software (TomoVision, Canada). The CSAs of each skeletal muscles (rectus abdominis, abdominal oblique, and erector spinae muscles), subcutaneous fat, and visceral fat were calculated with the function of region growing, 2D, and morphology.

A quantitative assessment of fat accumulation within skeletal muscle was achieved by calculating the percentage value of the fat fraction, which is the fat signal divided by the sum of the fat and water signals. We analyzed same MR image three times, and then averaged values for CSA and the percentage of intramuscular fat were used for analyses as reference. We used ImageJ software (Version 1.47v, National Institutes of Health, USA) to analyze all ultrasound images-as described in detail elsewhere (Tanaka et al. 2017). Echo intensities were expressed in arbitrary units (A.U.) on a scale of 0–255 (black = 0, white = 255). As we mentioned before, we acquired three EFOV ultrasound images from each skeletal muscle. The analyzed values of CSAs and echo intensities from those three EFOV ultrasound imaging were averaged and used for the statistical analyses. We also measured the thickness (Abe et al. 1994) of the subcutaneous fat just above each skeletal muscle three times for each image, and then averaged values are used for analyses.

Statistical analyses. We indicated all values as means and standard deviations (SDs). Since all measurement items were normally distributed (p values in the Shapiro-Wilk test were p>0.05), a one-way analysis of variance (ANOVA) was used to examine difference in CSA between MRI and EFOV ultrasound imaging. The Bland-Altman plot was used to confirm the existence of systematic errors. Pearson's product correlation with confidence interval (CI) was employed to investigate the relationship between accumulation of intramuscular fat by MRI and echo intensity by ultrasound imaging in each skeletal muscle group. Based on this simple regression equation, we estimated the percentage of fat accumulation by echo intensity for convenience. Then, the intraclass-correlation coefficients (ICC) were used to examine the coincidence between estimated and reference values of intramuscular fat accumulation in trunk. We also tried to find the parameter which has significant relation to MRI-derived intramuscular fat accumulation. In this analysis, we set following variables as the independent variables in the stepwise multiple regression analysis: echo intensity of each skeletal muscle, subcutaneous fat thickness just above each skeletal muscle, and waist circumference. Other stepwise multiple regression analyses were applied to examine the relationship between visceral fat and other parameters. In this case, we set followings as the dependent variables: waist circumference, body mass index, subcutaneous fat thickness just above each skeletal muscle, CSA and echo intensity of rectus abdominis, abdominal oblique, and erector spinae muscle. To check the multicollinearity, we calculated the variance inflation factor. We set the level of significance at $p<0.05$.

Results

The mean values (± SDs) of participants were as follows: age: 21.7 ± 4.0 years old, body mass index: 21.0 ± 1.8 kg/m^2, waist circumference: 75.5 ± 5.7 cm, and body fat: 16.4 ± 3.9%. The body mass index ranged between 18.2 and 24.8 kg/m^2 (Table 1). The averaged CSA values by MRI and EFOV ultrasound imaging were 13.5 cm^2 and 13.0 cm^2 for the rectus abdominis, 47.8 cm^2 and 48.4 cm^2 for the abdominal oblique, and 61.5 cm^2 and 61.3 cm^2 for the erector spinae. There were no significant differences in the

CSA measured by 2 methods (Figure 2). Figure 3 shows the relationships between CSA measured by MRI and that by EFOV ultrasound imaging. The slopes and intercepts of the regression equations for the relationship in CSA between MRI and EFOV ultrasound imaging were not significantly different from 1 and 0, respectively. In these correlations, $R^2 = 0.74$ ($0.72 \leq CI \leq 0.93$) for rectus abdominis, $R^2 =0.84$ ($0.83 \leq CI \leq 0.96$) for abdominal oblique, and $R^2 = 0.81$ ($0.79 \leq CI \leq 0.95$) for erector spinae muscle. The Bland-Altman plot (Bland and Altman 1986) showed no systematic errors between CSAs by MRI and EFOV ultrasound imaging ($0.07 \leq r \leq 0.14$). The values of lower and upper limits of agreement were -2.3 and 3.5 for rectus abdominis, -6.9 and 6.9 for abdominal oblique, and -7.1 and 8.5 for erector spinae. Regarding the muscle quality, all of the correlation coefficients between the accumulation of intramuscular fat by MRI and echo intensity by EFOV ultrasound imaging were significant in each skeletal muscle group. Namely, $r = 0.47$ ($0.13 \leq CI \leq 0.71$) for rectus abdominis, $r = 0.38$ ($0.02 \leq CI \leq 0.65$) for abdominal oblique, and $r = 0.37$ ($0.02 \leq CI \leq 0.65$) for erecter spinae (Figure 4). The pooled data showed the significant association between intramuscular fat accumulation and echo intensities of abdominal skeletal muscle groups ($r = 0.52$, $0.36 \leq CI \leq 0.66$, Figure 4). Then, to examine the reliability of echo intensity, we calculated the estimated value of the percentage of intramuscular fat accumulation in each skeletal muscle group based on the regression equation. Note that the regression equations have little meaning because the value of echo intensity changes depends on the setting of the ultrasonic device such as gain, frequency, ultrasound device itself, etc. As a result, the ICC values between the percentage of intramuscular fat accumulation measured by MRI and estimated by EFOV ultrasound imaging were as following: 0.36 ($0.01 \leq CI \leq 0.64$) for rectus abdominis, 0.29 ($0.08 \leq CI \leq 0.58$) for abdominal oblique, 0.27 ($0.09 \leq CI \leq 0.57$) for erector spinae, and 0.60 ($0.45 \leq CI \leq 0.72$) for pooled data. On the other hand, the stepwise multiple regression analysis indicated that echo intensity was the only significant predictor of MRI-derived intramuscular fat accumulation within each skeletal muscle group (Table 2). We also applied stepwise multiple regression analysis to investigate the existence of association between visceral fat area and other parameters. As a result, waist circumference and the echo intensity of the abdominal oblique muscle were selected as the significant predictor of the visceral fat area (Table 3). In other words, the values of subcutaneous fat thickness, echo intensity of rectus abdominis and erector spinae muscles had no significant relation to visceral fat. There was no effect of multicollinearity in regression analyses, namely, all variance inflation factors were below 10 (Table 2 and 3).

Discussion

The results of the present study demonstrated the validity of EFOV ultrasound imaging to assess the quantitative characteristics of abdominal skeletal muscles in healthy young men using MRI as a reference. The CSAs of the rectus abdominis, abdominal oblique, and erector spinae muscles measured by EFOV ultrasound imaging correlated and were not significantly different from those by MRI. Furthermore, no systematic errors were noted between the two measurement methods for CSAs. Regarding the accumulation of intramuscular fat, stepwise regression analyses indicated the echo intensities was the only significant predictor of fat accumulation within each trunk skeletal muscles. However, the correlation coefficients and ICC between the accumulation of intramuscular fat measured by MRI and that assessed by EFOV ultrasound imaging were significant but relatively low.

Previous studies reported the reliability of EFOV ultrasound imaging to assess the quantity and quality of skeletal muscle (e.g., Melvin et al. 2014 for the limbs; Tanaka et al. 2017 for the trunk). However, to the best of our knowledge, only Noorkoiv et al. (2010) compared CSA measurement values by EFOV ultrasound imaging to those by the gold standard (in their case, CT). They found that the reliability of EFOV ultrasound imaging was dependent on the section. Namely, as for the thigh, only the proximal-mid-thigh sections (30, 40 and 50% of the thigh length) were in the acceptable. They speculated that low reliability at the distal section was caused by angling of the ultrasound probe and the shape of the muscle. Certainly, the surfaces of the distal section of the thigh are not flat, difficulties are associated with moving the transducer without deviating from the original scanning plane. In the present study, the surface of the abdominal lateralis also slightly curved; however, the degree of the curve was not as steep as that of the thigh. Tanaka et al. (2017) also reported high reliability for measuring the abdominal oblique muscle. Therefore, there were no technical issues associated with the curved surface in the present study. The CSA of each skeletal muscle in the present study was similar to those reported previously using MRI as a reference (e.g., Tanaka et al. 2016): rectus abdominis, 6.2 cm^2 vs. 6.7 cm^2;

abdominal oblique, 29.3 cm^2 vs. 31.0 cm^2; erector spinae, 28.8 cm^2 vs. 29.9 cm^2.

This is the first study to report significant correlations between echo intensity by EFOV ultrasound imaging and intramuscular fat accumulation by MRI for trunk skeletal muscle groups. These relationships were significant but weak. ICC values between the reference and estimated values for the percentage of intramuscular fat were also relatively low. However, the stepwise multiple regression analysis identified echo intensity as the only significant predictor of MRI-derived intramuscular fat accumulation. Previous studies reported the echo intensity by traditional ultrasound imaging mainly reflects the degree of extracellular fat accumulation within skeletal muscle (e.g., Akima et al. 2016). Other previous studies reported that echo intensity by EFOV ultrasound imaging correlated with that by traditional ultrasound imaging (e.g., Jenkins et al. 2015). Based on these findings, echo intensity by EFOV imaging in this study may also reflect the degree of extracellular fat accumulation within skeletal muscle. However, the value of echo intensity is expressed in arbitrary units and is affected by differences in a number of factors, including the ultrasound device used, gain, frequency, and focus point. Therefore, the settings of the ultrasound device such as gain and frequency in the study may not have been optimal for assessing the quality of trunk skeletal muscles. Further studies are needed to select more appropriate ultrasound settings and/or other predictors in combination with echo intensity in order to evaluate trunk skeletal muscle quality by EFOV ultrasound imaging. It is also important to note that the highest fat percentage was in the abdominal oblique muscle, while the highest echo intensity was in the rectus abdominis muscle. Similar discrepant relationship between intramuscular fat accumulation and echo intensity were previously reported for the thigh (Melvin et al. 2014). However, the reason was not previously described. As for the present study, the fascia of the abdominal oblique muscle may have caused the diffuse reflection and attenuation of the echo. In other words, the echo intensity of the oblique muscle group may be decreased by averaging the echo intensities in the internal and external oblique muscles and transverse abdominal muscles. Another possibility was the effect of subcutaneous fat. Previous studies showed that greater subcutaneous fat accumulation was associated with reduced echo intensity (Young et al. 2015; Burton and Stock 2018). Further studies on obese individuals as subjects and/or ^{1}H magnetic resonance spectroscopy are needed to clarify the effects of subcutaneous fat on echo intensity in abdominal skeletal muscles.

As a novel approach using EFOV ultrasound imaging on trunk skeletal muscles, we attempted to evaluate its relation to visceral fat areas. Tanaka et al. (2019) previously indicated that changes in the visceral fat area altered the distribution of trunk skeletal muscle groups. Another study reported a correlation between the quality of trunk skeletal muscles and visceral fat (Maltais et al. 2018). In the present study, stepwise multiple regression analyses indicated that the CSA of visceral fat correlated with the echo intensity of the abdominal oblique muscle. Furthermore, adjusted R^2 became slightly higher (0.373 vs. 0.530) when the echo intensity of the abdominal oblique muscle was added as the dependent variable. These results are reasonable because the degree of fat accumulation within skeletal muscle was the highest in the abdominal oblique muscle. In national annual health check-ups in Japan, waist circumference at the height of umbilicus is used as one of the indicators for metabolic syndrome. However, this anthropometric method is not completely accurate because the measured value is the sum of tissues such as fat, bone, and skeletal muscle, and does not reflect the value of fat itself. To spread this novel index of the central obesity, i.e., the echo intensity of the abdominal oblique muscle, we need a further research with obese people as subjects.

More than 40% of the whole-body skeletal muscle mass is present in the trunk. In addition, trunk skeletal muscles are more sensitive to aging atrophy compared with the extremities (Ishida et al. 1997; Teichtahl et al. 2015). If EFOV ultrasound imaging becomes more widespread and a simple evaluation of abdominal skeletal muscles is possible, sarcopenia and metabolic syndrome may be diagnosed at earlier stages. However, there were some limitations in the present study. As described earlier, the relationships between echo intensities by EFOV ultrasound imaging and MRI-derived intramuscular fat accumulation were significant but weak. We only acquired data from young healthy men. We need to confirm the validity of EFOV ultrasound imaging of trunk skeletal muscles in women as well as in obese individuals and the elderly. Furthermore, we did not obtain information on the iliopsoas muscle group. Since the iliopsoas muscle located in a deep part of the trunk, we were unable to obtain clear images from some subjects. If we used the newest model of ultrasound imaging device, clear image of the iliopsoas muscle group may be acquired.

Summary

The present results demonstrated that EFOV ultrasound imaging is a valid method for evaluating CSA, in trunk skeletal muscles. As for the muscle quality, the associations between echo intensity and the accumulation of non-contractile tissue such as intramuscular fat were significant but relatively weak. The possibility of a correlation between visceral fat in and the echo intensity of the abdominal oblique muscle was preliminary indicated. To assess the trunk skeletal muscle quality by EFOV ultrasound imaging, further research is warranted to find better ultrasound setting and/or other predictor used with echo intensity. The validity of EFOV ultrasound imaging to assess the trunk skeletal muscle in women, obese individuals, and the elderly should also be clarified.

Acknowledgement

We thank for all participants of this study. We also appropriate Brain & Mind Research Center, Nagoya University. This study was funded by a Grant-in-Aid for Young Scientists (B) from the Japan Society for the Promotion of Science (17K13087).

References

Abe T, Kondo M, Kawakami Y, Fukunaga T. Prediction equations for body composition of Japanese adults by B-mode ultrasound. Am J Hum Biol 1994;6:161-170.

Akima H, Hioki M, Yoshiko A, Koike T, Sakakibara H, Takahashi H, Oshida Y. Intramuscular adipose tissue determined by T1-weighted MRI at 3T primarily reflects extramyocellular lipids. Magn Reson Imaging 2016;34: 397-403.

Ahtiainen JP, Hoffren M, Hulmi JJ, Pietikainen M, Mero AA, Avela J, Hakkinen K. Panoramic ultrasonography is a valid method to measure changes in skeletal muscle cross-sectional area. Eur J Appl Physiol 2010;108:273-279.

Bland JM, Altman DG. Statistical methods for assessing agreement between two methods of clinical measurement. Lancet 1986;327:307-310.

Burton AM, Stock MS. Consistency of novel ultrasound equations for estimating percent intramuscular fat. Clin Physiol Funct Imaging 2018; doi: 10.1111/cpf.12532.

Cruz-Jentoft AJ, Baeyens JP, Bauer JM, Boirie Y, Cederholm T, Landi F, Martin FC, Michel JP, Rolland Y, Schneider SM, Topinkova E, Vandewoude M, Zamboni M. Sarcopenia: European consensus on definition and diagnosis. Report of the European Working Group on Sarcopenia in Older People. Age and Aging 2010;39:412-423.

Cruz-Jentoft AJ, Bahat G, Bauer J, Boirie Y, Bruyère O, Cederholm T, Cooper C, Landi F, Rolland Y, Sayer AA, Schneider SM, Sieber CC, Topinkova E, Vandewoude M, Visser M, Zamboni M; Writing Group for the European Working Group on Sarcopenia in Older People 2 (EWGSOP2), and the Extended Group for EWGSOP2. Sarcopenia: revised European consensus on definition and diagnosis. Age Ageing 2019;48: 16-31.

Faul F, Erdfelder E, Buchner A, Lang AG. Statistical power analyses using G*Power 3.1: Tests for correlation and regression analyses. Behav Res Methods 2009;41: 1149-1160.

Hicks GE, Simonsick EM, Harris TB, Newman AB, Weiner DK, Nevitt MA, Tylavsky FA. Cross-sectional associations between trunk muscle composition, back pain, and physical function in the health, aging and body composition study. J Gerontol A Biol Sci Med Sci 2005;60:882-887.

Ido A, Nakayama Y, Ishii K, Iemitsu M, Sato K, Fujimoto M, Kurihara T, Hamaoka T, Satoh-Asahara N, Sanada K. Ultrasound-derived abdominal muscle thickness better detects metabolic syndrome risk in obese patients than skeletal muscle index measured by dual-energy x-ray absorptiometry. PLoS One 2015:23;10:e0143858.

Ishida Y, Kanehisa H, Carroll JF, Pollock ML, Graves JE, Ganzarella L. Distribution of subcutaneous fat and muscle thicknesses in young and middle-aged women. Am J Human Biol 1997;9:247-255.

Jenkins ND, Miller JM, Buckner SL, Cochrane KC, Bergstrom HC, Hill EC, Smith CM, Housh TJ, Cramer JT. Test-retest reliability of single transverse versus panoramic ultrasound imaging for muscle size and echo intensity of the biceps brachii. Ultrasound Med Biol 2015;41:1584-1591.

Landis JR, Koch GG. The measurement of observer agreement for categorical data. Biometrics 1977;33:159-174.

Lee CG, Boyko EJ, Barrett-Connor E, Miljkovic I, Hoffman AR, Everson-Rose SA, Lewis CE, Cawthon PM, Strotmeyer ES, Orwoll ES; Osteoporotic Fractures in Men (MrOS) Study Research Group. Insulin sensitizers may attenuate lean mass loss in older men with diabetes. Diabetes Care 2011;34:2381-2386.

Maltais A, Alméras N, Lemieux I, Tremblay A, Bergeron J, Poirier P, Després JP. Trunk muscle quality assessed by computed tomography: Association with adiposity indices and glucose tolerance in men. Metabolism 2018;85:205-212.

Melvin MN, Smith-Ryan AE, Wingfield HL, Fultz SN, Roelofs EJ. Evaluation of muscle quality reliability and racial difference in body composition of overweight individuals. Ultrasound Med &Biol 2014;40:1973-1979.

Noorkoiv M, Nosaka K, Blazevich AJ. Assessment of quadriceps muscle cross-sectional area by ultrasound extended-field-of-view imaging. Eur J Appl Physiol 2010;109:631-639

Pillen S, Arts IMP, Zwarts MJ. Muscle ultrasound in neuromuscular disorders. Muscle Nerve 2008;37:679-693.

Pillen S, Tak RO, Zwarts MJ, Lammens MM, Verrijp KN, Arts IM, van der Laak JA, Hoogerbrugge PM, van Engelen BG, Verrips A. Skeletal muscle ultrasound: correlation between fibrous tissue and echo intensity. Ultrasound Med Biol 2009;35:443-446.

Reimers K, Reimers CD, Wagner S, Paetzke I, Pongratz DE. Skeletal muscle sonography: a correlative study of echogenicity and morphology. J Ultrasound Med 1993;12:73-77.

Rosenberg JG, Ryan ED, Sobolewski EJ, Scharville MJ, Thompson BJ, King GE. Reliability of panoramic ultrasound imaging to simultaneously examine muscle size and quality of the medial gastrocnemius. Muscle Nerve2014; 49:736-740.

Ryan AS, Harduarsingh-Permaul AS. Effects of weight loss and exercise on trunk muscle composition in older women. Clin Interv Aging 2014;9:395-402.

Sachs S, Zarini S, Kahn DE, Harrison KA, Perreault L, Phang T, Newsom SA, Strauss A, Kerege A, Schoen JA, Bessesen DH, Schwarzmayr T, Graf E, Lutter D, Krumsiek J, Hofmann SM, Bergman BC. Intermuscular adipose tissue directly modulates skeletal muscle insulin sensitivity in humans. Am J Physiol Endocrinol Metab 2019;316:E866-E879.

Tanaka NI, Miyatani M, Masuo Y, Fukunaga T, Kanehisa H. Applicability of a segmental bioelectrical impedance analysis for predicting the whole body skeletal muscle volume. J Appl Physiol 2007;103:1688-1695.

Tanaka NI, Murakami H, Ohmori Y, Aiba N, Morita A, Watanabe S, Miyachi M. Association of visceral fat with abdominal skeletal muscle distribution in overweight Japanese. Obes Res Clin Pract 2018;12:378-383.

Tanaka NI, Ogawa M, Yoshiko A, Ando R, Akima H. Reliability of size and echo intensity of abdominal skeletal muscles using extended field-of-view ultrasound imaging. Eur J Appl Physiol. 2017;117:2263-2270.

Tanaka NI, Yamada M, Tanaka Y, Fukunaga T, Nishijima T, Kanehisa H. Difference in abdominal muscularity at the umbilicus level between young and middle-aged men. J Physiol Anthropol. 2007;26:527-532.

Teichtahl AJ, Urquhart DM, Wang Y, Wluka AE, Wijethilake P, O'Sullivan R, Cicuttini FM. Fat infiltration of paraspinal muscles is associated with low back pain, disability, and structural abnormalities in community-based adults. Spine 2015;15:1593-1601.

Young HJ, Jenkins NT, Zhao Q, Mccully KK. Measurement of intramuscular fat by muscle echo intensity. Muscle Nerve 2015;52:963-971.

Figure captions

Figure 1. Typical examples of abdominal MRI using the fat-water separated two-point Dixon imaging technique (upper panels) and analyzed images by EFOV ultrasound imaging for the CSAs and echo intensities (lower 3 panels). A: rectus abdominis, B: abdominal oblique, C: erector spinae muscles.

Figure 2. Comparison of CSAs by MRI and EFOV ultrasound imaging.

Figure 3. Correlations in CSAs between MRI and EFOV ultrasound imaging (left panels) and Bland-Altman plots (right panels). In left panels, solid lines are for regressions; dotted lines are for y = x. In right panels, y axis indicated residual (CSA measured by MRI minus that by EFOV ultrasound imaging). x axis was the average of CSA by two methods. ~~s~~Solid lines are for y = 0, dotted lines are for limits of agreement.

Figure 4. Relationships between accumulation of intramuscular fat measured by MRI and echo intensities measured by EFOV ultrasound imaging. Upper panel is for result for rectus abdominis, abdominal oblique, and erector spinae muscles, respectively. The regression equations were $y = 0.16 \times$ echo intensity -0.61 for rectus abdominis, $y = 0.145 \times$ echo intensity $+3.59$ for abdominal oblique, and $y = 0.11 \times$ echo intensity $+ 2.40$ for erector spinae. Lower panel is for pooled data. In this case, the regression equation was $y = 0.14 \times$ echo intensity $+ 2.16$. In both panels, solid lines are for regressions.

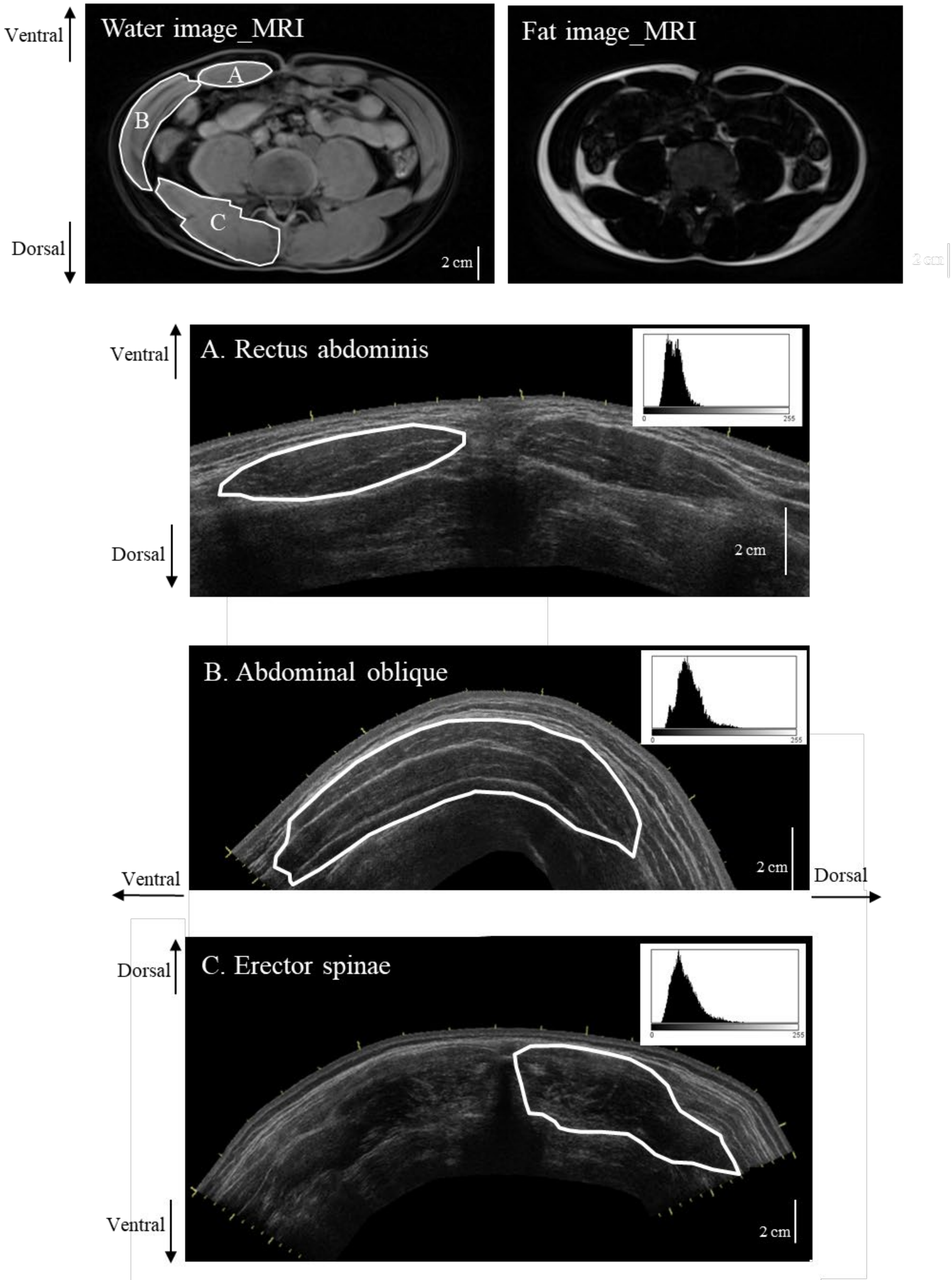
Ventral
Dorsal
Water image_MRI
A
B
C
2 cm
Fat image_MRI
2 cm
Ventral
Dorsal
A. Rectus abdominis
0
255
2 cm
B. Abdominal oblique
0
255
Ventral
2 cm
Dorsal
Dorsal
C. Erector spinae
0
255
Ventral
2 cm

Figure 1

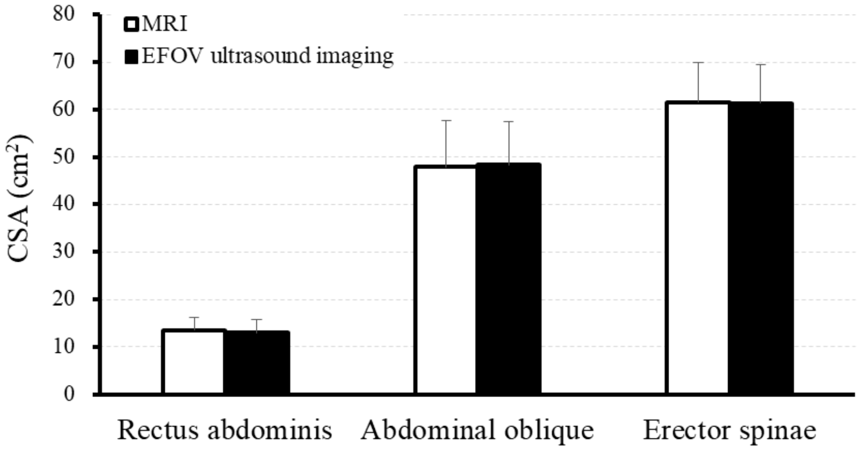
MRI
EFOV ultrasound imaging
CSA (cm^2)
0
10
20
30
40
50
60
70
80
Rectus abdominis
Abdominal oblique
Erector spinae

Figure 2

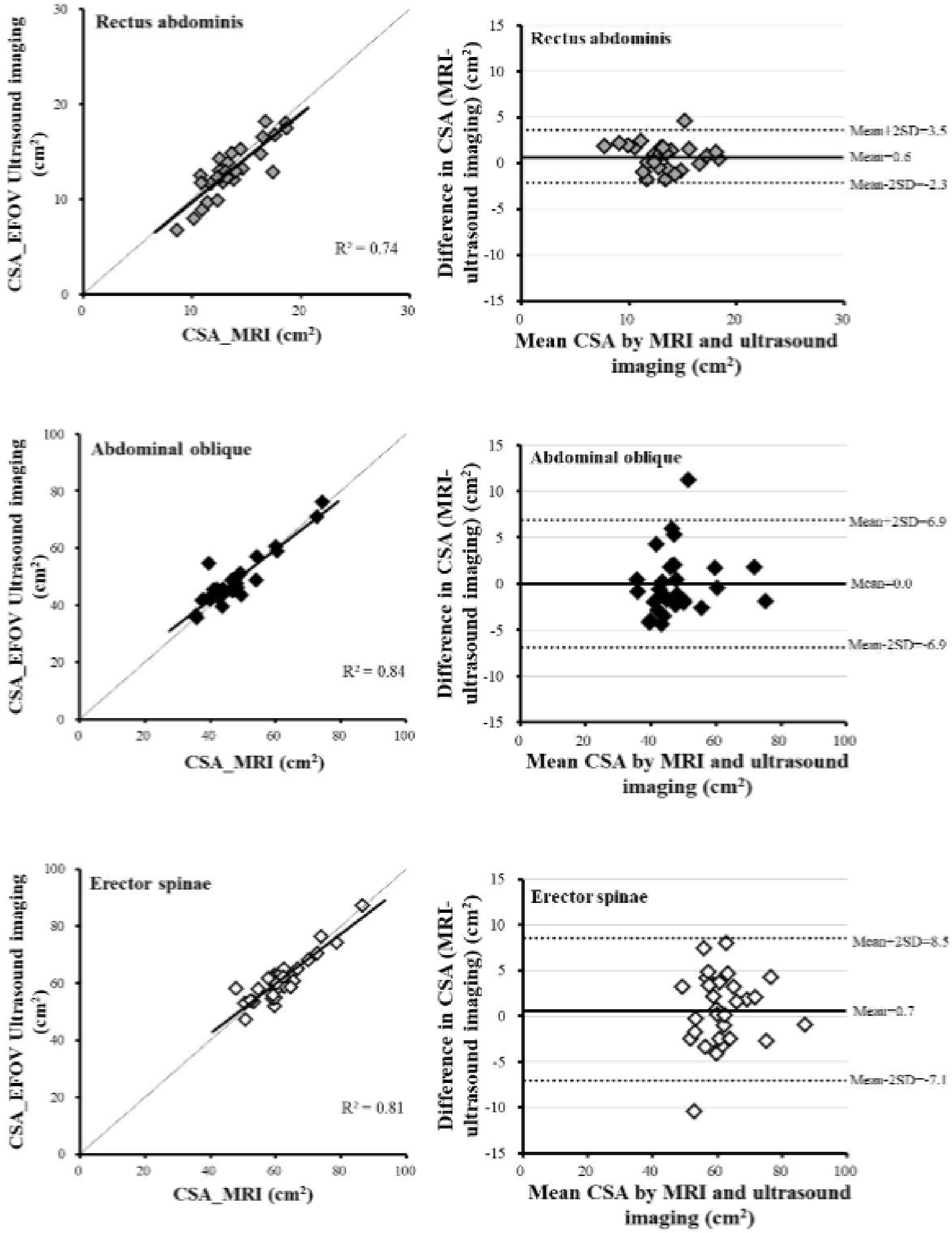
Rectus abdominis
CSA_EFOV Ultrasound imaging (cm²)
CSA_MRI (cm²)
0
10
20
30
R² = 0.74
Rectus abdominis
Difference in CSA (MRI-ultrasound imaging) (cm²)
Mean CSA by MRI and ultrasound imaging (cm²)
15
10
5
0
-5
-10
-15
Mean+2SD=3.5
Mean=0.6
Mean-2SD=-2.3
Abdominal oblique
CSA_EFOV Ultrasound imaging (cm²)
CSA_MRI (cm²)
0
20
40
60
80
100
R² = 0.84
Abdominal oblique
Difference in CSA (MRI-ultrasound imaging) (cm²)
Mean CSA by MRI and ultrasound imaging (cm²)
Mean+2SD=6.9
Mean=0.0
Mean-2SD=-6.9
Erector spinae
CSA_EFOV Ultrasound imaging (cm²)
CSA_MRI (cm²)
R² = 0.81
Erector spinae
Difference in CSA (MRI-ultrasound imaging) (cm²)
Mean CSA by MRI and ultrasound imaging (cm²)
Mean+2SD=8.5
Mean=0.7
Mean-2SD=-7.1

Figure 3

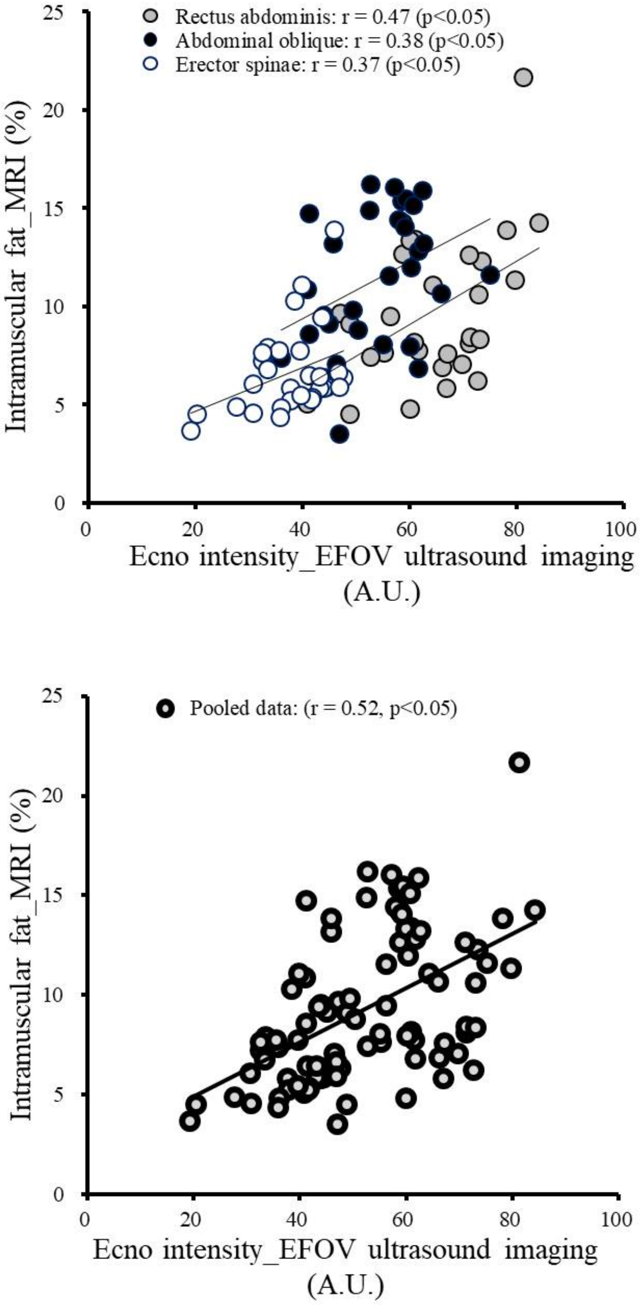
Rectus abdominis: r = 0.47 (p<0.05)
Abdominal oblique: r = 0.38 (p<0.05)
Erector spinae: r = 0.37 (p<0.05)
Intramuscular fat_MRI (%)
25
20
15
10
5
0
0
20
40
60
80
100
Ecno intensity_EFOV ultrasound imaging (A.U.)
Pooled data: (r = 0.52, p<0.05)
Intramuscular fat_MRI (%)
25
20
15
10
5
0
0
20
40
60
80
100
Ecno intensity_EFOV ultrasound imaging (A.U.)

Figure 4

Table 1. Morphological characteristics of subjects.

Items	Mean	SD	Min	Max
Age (yrs)	21.7	4.0	18.0	36.0
Height (cm)	172.7	5.9	160.7	186.7
Weight (kg)	62.6	7.0	50.7	81.2
Body mass index (kg/m^2)	21.0	1.8	18.2	24.8
Waist circumference (cm)	75.5	5.7	65.3	89.4
Body fat (%)	16.4	3.9	9.3	24.8
Cross-sectional area (cm^2)				
Rectus abdominis	13.5	2.6	8.6	18.7
Abdominal oblique	47.8	9.7	35.6	74.3
Erector spinae	61.5	8.4	47.8	86.5
Intramuscular fat (%)				
Rectus abdominis	9.8	3.7	4.5	21.6
Abdominal oblique	11.4	3.5	3.5	16.2
Erector spinae	6.6	2.2	3.7	13.9

Table 2. Results of stepwise multiple regression analyses as MRI-derived intramuscular fat accumulation for the dependent variables (%).

Dependent variables	Independent variables	Partial regression coefficient	Standard error	Confidence interval	P value	Standardized partial regression coefficient	Adjusted R^2	Variance inflation factor
Intramuscular fat_rectus abdominis	Echo intensity	0.16	0.06	0.04-0.28	<0.01*	0.47	0.19	1.00
	CSA	-	-	-	0.77	-	-	1.11
	Subcutaneous fat thickness	-	-	-	0.18	-	-	1.02
	Waist circumference	-	-	-	0.47	-	-	1.07
Intramuscular fat_abdominal oblique	Echo intensity	0.18	0.07	0.04-0.31	<0.01*	0.45	0.17	1.00
	CSA	-	-	-	0.46	-	-	0.36
	Subcutaneous fat thickness	-	-	-	0.95	-	-	1.04
	Waist circumference	-	-	-	0.42	-	-	1.00
Intramuscular fat_erector spinae	Echo intensity	0.11	0.05	0.004-0.22	<0.01*	0.37	0.11	1.00
	CSA	-	-	-	0.34	-	-	1.05
	Subcutaneous fat thickness	-	-	-	0.74	-	-	1.00
	Waist circumference	-	-	-	0.66	-	-	1.00

Echo intensity, corresponding muscle's echo intensity; CSA, cross-sectional area of corresponding muscle measured by EFOV ultrasound imaging; Subcutaneous fat thickness, measured just above the corresponding muscle; *, $p<0.05$

Table 3. Results of stepwise multiple regression analyses as MRI-derived visceral fat area for the dependent variable (cm^2).

Independent variables	Partial regression coefficient	Standard error	Confidence interval	P value	Standardized partial regression coefficient	Adjusted R^2	Variance inflation factor	Standard error of estimate
Model 1								
Waist circumference	1.98	0.44	1.09-3.07	<0.01*	0.67	0.41	1.00	13.40
Model 2								
Waist circumference	2.02	0.39	1.22-2.83	<0.01*	0.67	0.53	1.00	11.92
Echo intensity of abdominal oblique	0.72	0.25	1.99-1.23	<0.01*	0.37			
Body mass index	-	-	-	0.19	-	-	3.53	-
Subcutaneous fat above rectus abdominis	-	-	-	0.37	-	-	1.07	-
Subcutaneous fat above abdominal oblique	-	-	-	0.68	-	-	1.11	-
Subcutaneous fat above erector spinae	-	-	-	0.59	-	-	1.03	-
CSA of rectus abdominis	-	-	-	0.63	-	-	1.22	-
CSA of abdominal oblique	-	-	-	0.34	-	-	1.73	-

CSA of erector spinae	-	-	-	0.90	-	-	1.27	-
Echo intensity of rectus abdominis	-	-	-	0.22	-	-	1.37	-
Echo intensity of erector spinae	-	-	-	0.17	-	-	1.48	-

*, $p<0.05$